Optical Fiber pH Sensors Based on PAni-Coated Microstructured Optical Fibers

Armando Rodriguez, Guilherme Lopes, Jan Nedoma, *Senior Member, IEEE*, Sónia O. Pereira, António J. S. Fernandes, Raphael Jamier, Philippe Roy, Mikel Bravo, Manuel Lopez-Amo, *Senior Member, IEEE*, and Carlos Marques, *Member, IEEE*

***Abstract*—In this article, we report the analysis of a novel optical fiber pH sensor based in polyaniline (PAni) coating applied on a trenched core-free (only-bridge) silica fiber. The results are compared to another pH sensor based on side-polished silica fiber. The pH-sensitive polymer is synthesized over the fiber sample by means of oxidative polymerization, keeping records of the time where the reaction occurs to improve the sensitivity. The response to pH is enhanced in the case of the trenched core-free bridge fiber due to the higher interaction of the evanescent field with the PAni film and, thus, the surrounding media. The sensitivity in the linear zone of operation is 1.1 mW/pH, and a total transmittance of 55% in the pH range is 4.2–8.1. The repeatability of both sensors was checked, showing a high capability to perform studies in liquid samples due to its temperature independence, good sensitivity, and long-term stability.**

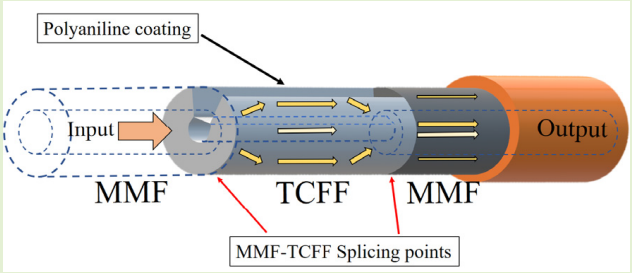

***Index Terms*— pH sensor, polyaniline (PAni), side-polished fiber, trenched core-free fiber (TCFF).**

I. Introduction

THE pursuit of efficient, accurate, and versatile sensing technologies is an important issue in various scientific and industrial domains. Among these, pH sensing stands out as a main parameter influencing diverse fields such as environmental monitoring, biomedical research, and chemical process control [1]. Monitoring pH is crucial for many applications, particularly in environmental and water quality assessment. Conventional methods, such as using pH electrodes, have several drawbacks, including signal drifts, membrane issues, and the need for frequent calibration. Optical fiber sensors have emerged as promising candidates for pH monitoring due to their inherent advantages including high sensitivity, immunity to electromagnetic and chemical interrelation, and remote operation capabilities.

Several techniques have been developed to meet this common demand for ease. In recent years, different types of sensors have been reported, mostly based on carbon nanotubes [2], potentiometric and capacitive changes [3], [4], [5], microelectrical–mechanical systems [6], CMOS [7], and surface plasmon resonance [8], [9], as the representative examples.

Optical fibers have been employed as a passive transmission line in a number of the previously discussed techniques (only to transfer light to and from the detecting head [10]), but in a large number of other techniques, they play an active role as optical transducers [11], [12], [13].

A key challenge in developing highly sensitive optical fiber pH sensors is achieving sufficient interaction between the guided light and the pH-sensitive coating material in the optical fiber. An optical fiber-embedded smart wound bandage fabricated using a polydimethylsiloxane (PDMS) precursor doped with rhodamine B dye, for the simultaneous assessment

Manuscript received 20 May 2024; revised 21 June 2024; accepted 24 June 2024. Date of publication 10 July 2024; date of current version 15 August 2024. This work was supported in part by MCIN/AEI/10.13039/501100011033 under Project PID2022-137269OB-C21 and Project TED2021-130378B-C22; in part by the Fondo Europeo de Desarrollo Regional (FEDER) "A way to make Europe;" in part by the European Union "Next Generation EU"/PRTR; in part by Beatriz Galindo in MICINN under Grant BEAGAL18/00116; in part by the CICECO–Aveiro Institute of Materials under Project LA/P/0006/2020, Project UIDB/50011/2020, and Project UIDP/50011/2020; in part by i3N under Project UIDB/50025/2020, Project UIDP/50025/2020, and Project LA/P/0037/2020; in part by DigiAqua under Project PTDC/EEI-EEE/0415/2021; in part by the National Funds through the Portuguese Science and Technology Foundation/MCTES (FCT I.P., Portugal); in part by the European Union through the Research Excellence For Region Sustainability and High-Tech Industries (REFRESH) under Project CZ.10.03.01/00/22_003/0000048 via the Operational Program Just Transition; and in part by the Ministry of Education, Youth, and Sports of the Czech Republic through the VSB–Technical University of Ostrava under Grant SP2024/081 and Grant SP2024/059. Open access funding provided by Universidad Pública de Navarra. The associate editor coordinating the review of this article and approving it for publication was Dr. Xuehao Hu. *(Corresponding author: Armando Rodriguez.)*

Please see the Acknowledgment section of this article for the author affiliations.

Digital Object Identifier 10.1109/JSEN.2024.3419257

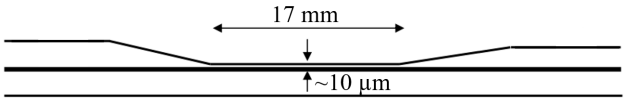

Fig. 1. Profile of D-shape optical fiber.

of pressure and pH and monitoring of the healing stage and condition on the wound region, was reported by Leal-Junior et al. [14]. The polyaniline (PAni) coating has garnered significant attention due to the good properties of the polymer, such as reversible pH-dependent conductivity and ease of synthesis. For instance, sensors based on PAni and fiber Bragg gratings (FBG), tilted FBG and long-period gratings, have been reported by Cheng et al. [15]. Specifically, a fiber-optic pH sensor was developed [16] based on tilted FBG where a coating of PAni was deposited on the fiber's surface, achieving a range of measurement of 2–12 with a fast response.

Another optical fiber sensing structure used is the D-shape optical fiber, where a section of the fiber's cladding is polished, exposing the core of this region [17]. This design enhances the interaction of light with the medium to be sensed. Several methods refer to optical fibers geometrically modified, such as fibers without cladding, but their sensitivity is compromised in most cases. D-shaped fibers have attracted the attention of researchers as a mechanically stronger structure for sensing [18].

In this article, we present a comprehensive comparative analysis of two different fiber-optic pH sensors, each one employing a distinct configuration and structure. We will explore the use of novel optical fiber structures, specifically a sensor based on an only-bridge-trenched core-free fiber (TCFF) combined with PAni coating. This type of microstructured optical fiber (MOF) can enhance the evanescent field interaction compared to conventional fiber geometries. We will compare its performance with a similar coating of an optical fiber sensor based on a D-shaped optical fiber.

II. Materials and Methods

The study was performed using two different types of sensing optical fibers that provide a platform for efficient light coupling and interaction with the surrounding medium. The first sensor system is based on a side-polished optical fiber from Phoenix Photonics,[1] also called D-shape as the structure formed in the fiber cladding. The aim is to remove a section of the cladding to gain access to the evanescent field. The polished region length is ∼17 mm, following a fiber profile as the one depicted in Fig. 1.

The other one is a TCFF manufactured by XLIM Institute (France), which has a particular inner structure. It consists of a coreless fiber where a longitudinal portion of cladding is removed, leaving a thin interface between the center of the optical fiber and the external medium that resembles a small suspended bridge. Fig. 2 depicts the microscope picture of the fiber and its dimensions.

The open space in the cladding makes it suitable for depositing smart materials or introducing elements to be measured,

[1]Registered trademark.

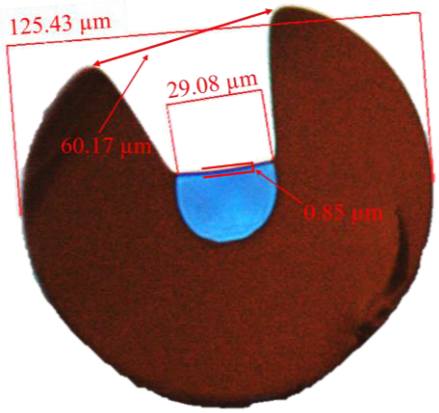

Fig. 2. Microscope photography of TCFF.

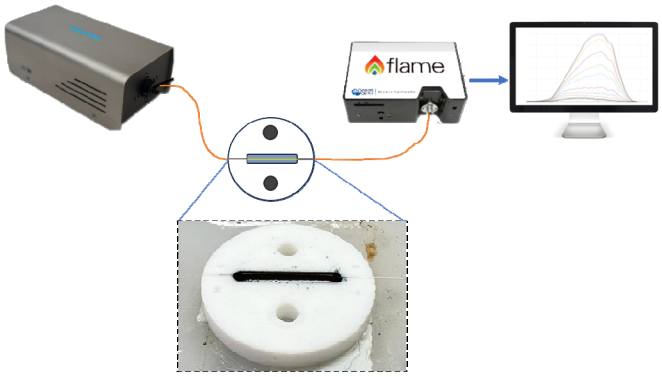

Fig. 3. Experimental setup of the novel fiber-optic pH sensor.

interacting with the light traveling either through the hollow core or the cladding.

In both experiments, corresponding to the two different optical fibers, the same transmissive setup was used, as shown in Fig. 3, where a Teflon container acts as a fiber holder allowing the PAni section deposited on the optical fiber to be immersed in the solution to be measured. A halogen light source model LSW7, brand *Sarspec*, has been used, whose maximum power is 7 W with an emission range between 380 and 2500 nm. The detector is a FLAME-T-UV-vis spectrometer manufactured by *Ocean Optics*, with a detection range of 180–890 nm, and the error margin according to the power resolution is 0.01 counts. The data were captured via the OceanView spectral analysis software and the traces were processed on a customized software developed in MATLAB.

The D-shape optical fiber was manufactured in a single-mode fiber (SMF) according to technical specification and connected through an FC-APC optical fiber pigtail on both ends. Both the spectrometer and halogen lamp source have SMA connectors in the interfaces with an SMA to FC-PC multimode fiber (MMF) pigtail attached. Thus, an additional APC-PC pigtailed transition was used.

In addition, the TCFF was spliced to an MMF pigtail in both ends, because of its internal diameter of ∼30 μm, being an optimal way to couple the light from the source and to retrieve its transmission spectrum.

A. PAni Synthesis

As stated before, PAni was used as the sensitive element to pH variations. This is a polymer that exhibits reversible

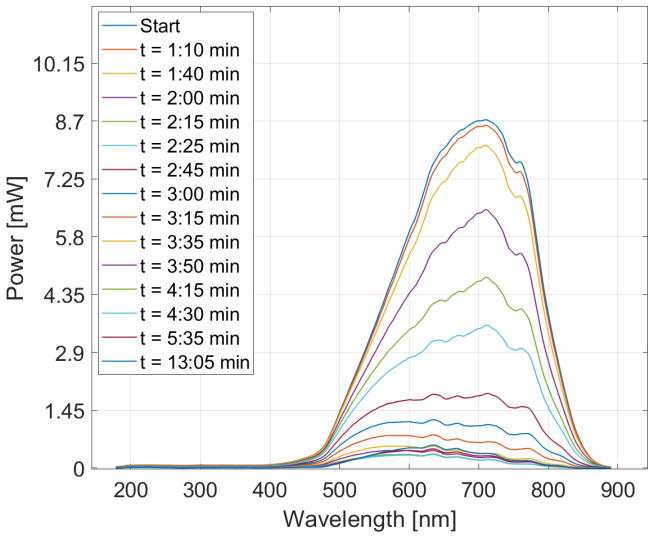

Fig. 4. Spectral evolution of TCFF during polymer synthesis on its surface.

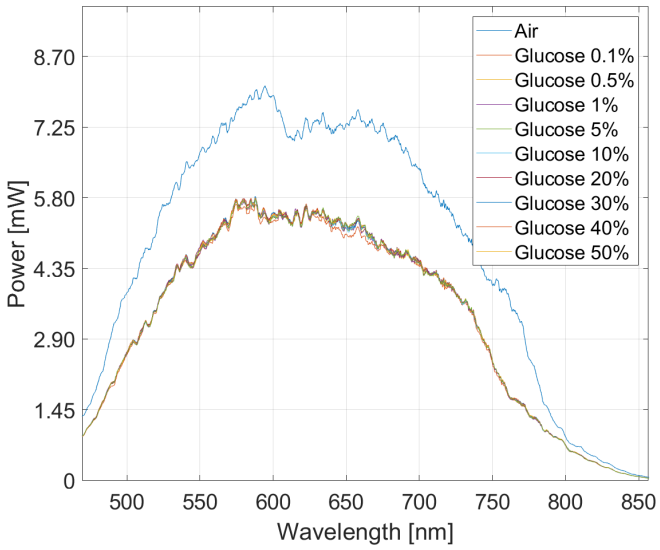

Fig. 5. Spectral response of bare D-shape optical fiber to RI variation.

pH-dependent conductivity, meaning that its electrical conductivity changes in response to variations in pH levels. Three oxidation states of PAni have been identified and all of these structures can exist either in their salt form (protonated) or in their base form (deprotonated), which is accomplished by applying the base form to an acid, as demonstrated in [16], [19], and [20].

The PAni layer was synthesized in situ by oxidative polymerization, i.e., in the presence of the D-shape optical fiber or the TCFF. The procedure was adapted from the work developed by Lopes et al. [17]. For this purpose, aniline was used as monomer and ammonium persulfate as an oxidizing agent in an acidic aqueous solution. Once fixed to the container, which had an estimated capacity of about 400 μL, the surface of the optical fiber is first cleaned with deionized water. Second, 300 μL of hydrochloric acid (HCl) at 1.0 M containing aniline (0.133 M) was poured into the container. Subsequently, 100 μL of a solution of ammonium persulfate (0.4 M) prepared with HCl (1.0 M) was added. By thoroughly mixing the solution, the reaction started immediately, rapidly turning from transparent to dark green color.

The polymerization time allows to optimize the thickness of the PAni film on the optical fiber; thicker may be more sensitive but leads to a slower response or stabilization. Therefore, hysteresis can be observed in the rise and fall of pH levels, as reported elsewhere [17]. In this work, a polymerization time of around 13 min was applied in ambient temperature conditions. For example, Fig. 4 depicts the spectral evolution of the TCFF during the PAni synthesis where the spectral intensity is expressed in terms of optical power (mW).

Finally, after the elapsed time, the excess polymer present in the recipient was removed and the coated optical fiber was washed with deionized water to ensure the complete elimination of reaction precursors.

B. Preparation of pH Samples

The experimental tests were carried out using solutions with different pH values. The samples were prepared by varying the ratio between sodium phosphate dibasic heptahydrate ($Na_2HPO_4 \cdot 7H_2O$, Sigma-Aldrich) and sodium phosphate monobasic monohydrate ($NaH_2PO_4 \cdot H_2O$, Sigma-Aldrich), keeping a constant concentration of 0.01 M. The phosphate ions were dissolved in a solution containing 0.137-M sodium chloride (NaCl) and 0.027-M potassium chloride (KCl). Eight solutions were calculated to maintain the ionic strength in all cases, with pH ranging from 2 to 10. The actual values were measured via pH electrode from Hanna Instruments, where the lowest sample recorded pH was 2.75 and the highest was 8.9.

The reference values of each test were measured by placing the coated optical fibers in a solution of HCl (0.1 M) for more than 5 min and capturing the spectrum. Afterward, the HCl was taken out and the initial sample of calculated pH is added. The procedure is repeated for all pH samples. All tests were performed in a controlled ambient room, with a constant temperature of 23 °C. Moreover, the refractive index (RI) of the solutions was measured and it was confirmed that all the samples present the same RI.

III. Results and Discussion

A. Characterization of Optical Fibers Without PAni

The optical fibers were tested before applying the polymer coating in order to check the sensitivity to RI and pH variations. With the aim of characterizing the response of the bare fibers, nine solutions of glucose with different RI were prepared by varying the concentration from 0.1% to 50% w/v, with RI unit (RIU) values from 1.332 to 1.3861. The RIU values were measured with an Easy R40 instrument from *Mettler Toledo*, which has a measurement range from 1.30 to 1.72 RIU and an accuracy of ±0.0001 RIU. As a reference, the RI of air was taken (∼1.000).

Fig. 5 represents the transmission spectrum evolution of the D-shape fiber without coating. The transition from air to glucose solutions is obvious, however, changing the RIU does not significantly affect the intensity of the spectrum. The TCFF was also tested and its response was similar.

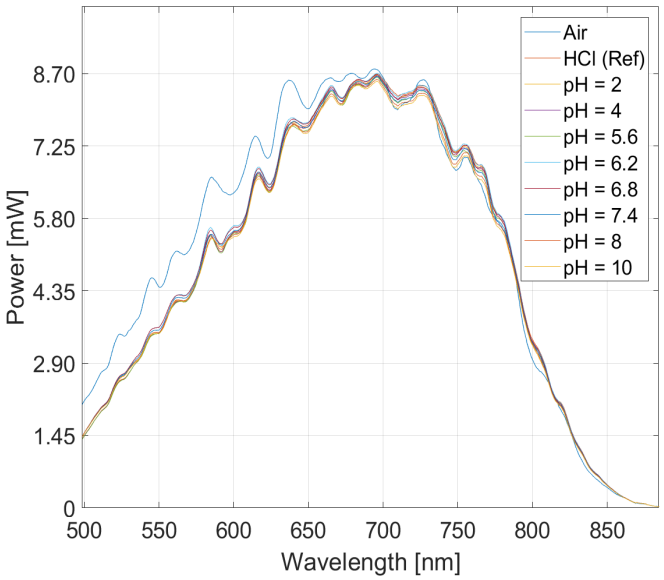

Fig. 6. Spectral response of bare TCFF to pH variation.

Moreover, the sensitivity of bare fibers to pH was also tested. Different pH solutions were used and the spectral response of TCFF is depicted in Fig. 6, where almost no changes in power level are achieved. A similar behavior was observed for the D-shape fiber.

In summary, both optical fibers without the polymer coating demonstrated no substantial reaction to changes in RI and pH. Nevertheless, the sample solutions used in the further experiments were carefully checked to have the same RI value.

B. Measurement of pH With PAni Coating

The tests were performed by placing the coated optical fibers in several pH solutions from the HCl reference sample to pH 9. Each pH solution was placed in the container, and after 4∼5 min of stabilization, the data were recorded. As the measurements are based on power variations, it is important to check the stability of the light sources used before each experiment.

First, the TCFF-based sensor was tested and the spectra show a peak around 634.5 nm, decreasing with the increase of pH. This peak was monitored showing only a slight variation up to pH = 4.2 after which the response suddenly increases with an approximate linear trend before getting a slow decreasing rate at the end of the test. The overall response resembles an "S" shape as can be observed in Fig. 7, after performing a sigmoid fitting to the peak intensity curve, where ∼99.25% (R^2) of the fit curve represents the actual sensor response. The inset figure depicts the spectral evolution caused by the pH variation.

This mathematical approach typically involves fitting parameters such as the saturation level, slope, and inflection point of the curve [21]. Moreover, it helps to understand valuable insights into the sensor's characteristics, such as its dynamic range, sensitivity, and response kinetics. Thus, the sensitivity value represents how much the response changes with respect to a change in the pH.

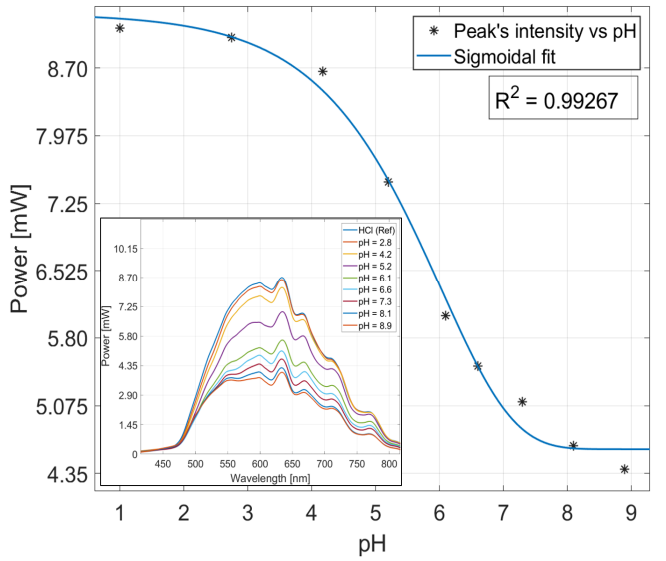

Fig. 7. Response of PAni-coated TCFF sensor to pH variations (inset: spectral evolution).

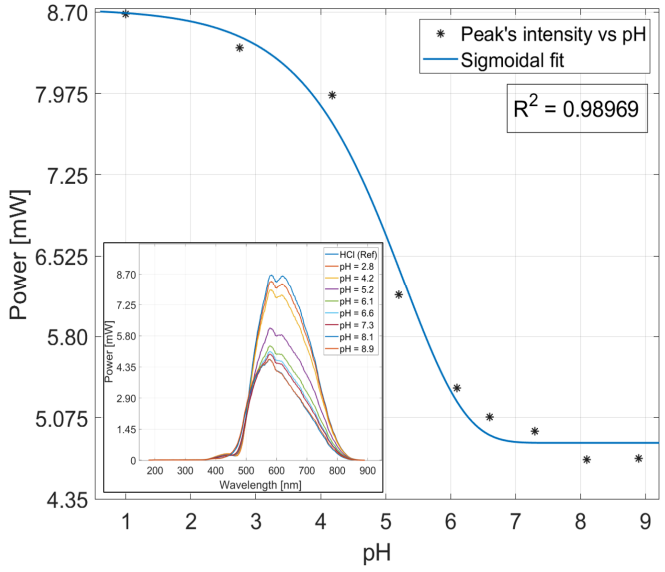

Fig. 8. Response of PAni-coated D-shape sensor to pH variations (inset: spectral evolution).

Based on this result, the optimal range of operation of this sensor can be defined from pH 4.2 to 8.1, where a linear trend was observed. The obtained sensitivity was about 1.06 mW/pH ($R^2 = 0.9604$).

Finally, the D-shape fiber-based sensor was also tested. This time, the polymer coating produced a peak of around 583.4 nm (see the inset of Fig. 8). The response is similar to the previous sensor, showing ∼98.97% of agreement to the sigmoidal fit, as depicted in Fig. 8. A linear trend range is also observed but this time between 2.75 and 6.8 ($R^2 = 0.9542$). A 0.95-mW/pH sensitivity was achieved in this configuration.

Although the optimal measurement range is different than the case of TCFF sensor, these results are useful for several applications, including the survival of aquatic life.

C. Repeatability Test

The experimental procedures were repeated to assess the suitability of the sensor for multiple uses. Several tests were

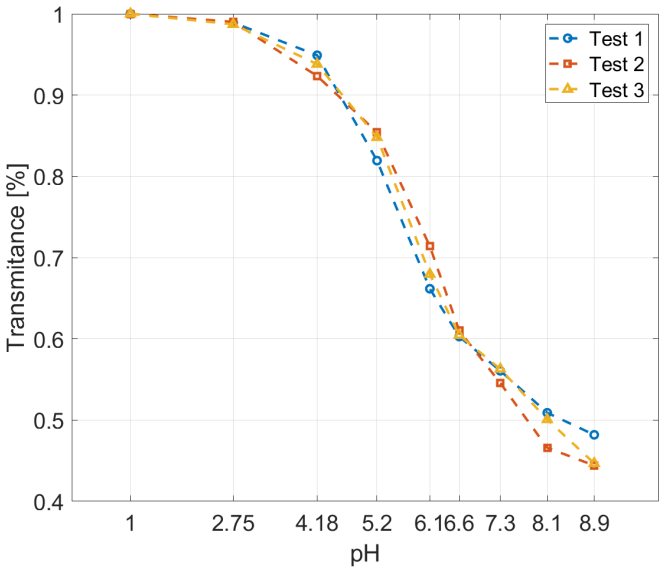

Fig. 9. Repeatability of the TCFF-based sensor.

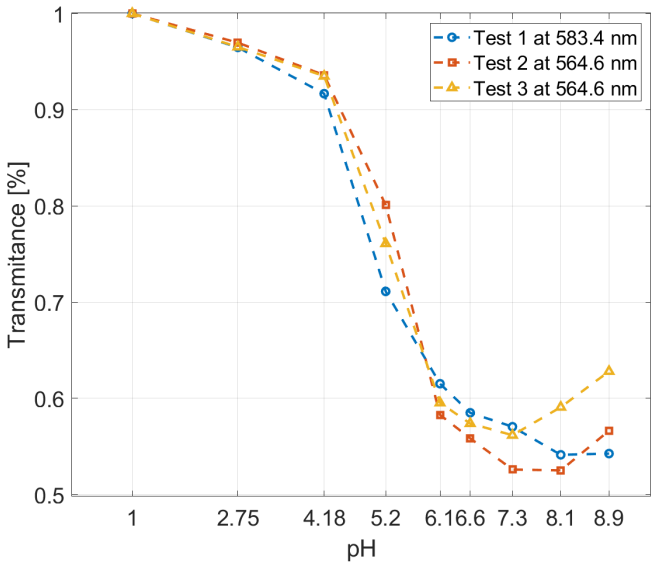

Fig. 10. Normalized transmittance analysis of the repeatability test in D-shape fiber-based sensor.

carried out with a day gap between every measurement. After finishing each of them, the sensor was rinsed with plenty of deionized water and stabilized using a 0.1-M solution of HCl.

As demonstrated in [17], the PAni polymer film has shown a high hysteresis when decreasing steps of pH levels. Therefore, the measurement in this work was only performed in increasing steps. Several reports support the findings, stating that this issue is related to different protonation/deprotonation rates in the polymerization of PAni [22].

As a merit figure in the analysis, the normalized transmittance of the sensor was studied for both the initial and the repeatability tests. These showed the same transmittance trend after two days of polymer synthesis.

The peak intensity of spectral response remained at 634.6 nm, and despite a decrease in the intensity, the sensor response remained very close. A sensitivity of 1.064 mW/pH ($R^2 = 0.9803$) and 0.951 mW/pH ($R^2 = 0.9674$) was determined for subsequent tests 2 and 3, respectively. Fig. 9 depicts the plot of the experimental results where the optimal operation zone (linear response) was similar in all cases.

The same procedure was repeated with the D-shape fiber-based sensor as well. While the overall sensor transmittance trend remained similar up to pH 7.3 across the repeated tests, there were some notable deviations at higher pH values (see Fig. 10). Specifically, in the initial test, the normalized transmittance continued decreasing with increasing pH above 7.3. However, in subsequent tests 2 and 3, the spectral response peaked shifted to a lower wavelength of 564.6 nm, and the transmittance began increasing again for pH $>$ 7.3.

To quantify this effect, the percent change in normalized transmittance between pH 7.3 and 8.9 for each test was calculated. In the initial test, there was a 12.6% decrease, but in tests 2 and 3, the transmittance increased by 7.8% and 9.2%, respectively, over that pH range.

As can be observed, both sensors achieved a similar trend in the linear operation zone. However, the sensor based on D-shape optical fiber shows inconsistent behavior at high pH levels. In the case of the sensor with TCFF, the response was enhanced in comparison to the first test, which makes it a suitable candidate for multiple usages.

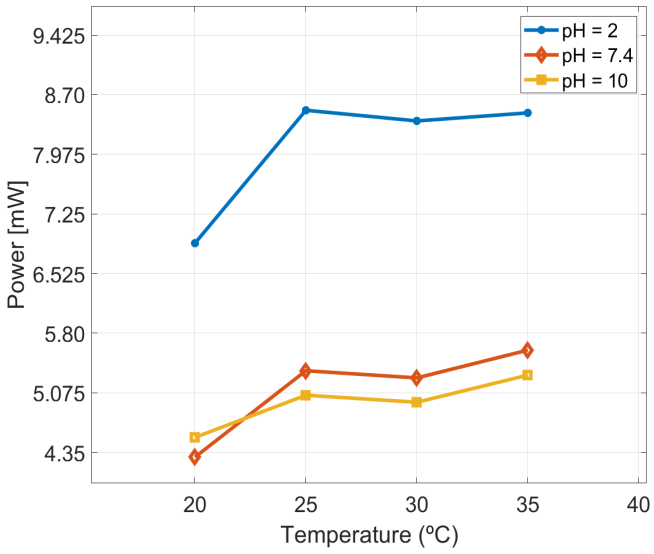

Fig. 11. Temperature variation influence in TCFF-based sensor.

D. Cross-Sensitivity Test

The previous experimental tests were carried out in a controlled laboratory environment, around 23 °C. The behavior of the sensor was also tested at different temperature values around that, using three pH levels (2, 7.4, and 10). For this purpose, a climatic chamber was used to perform a temperature sweep from 20 °C to 35 °C, in steps of 5 °C. The measurement was recorded with a stabilization time of approximately 10 min between each one, ensuring that both the chamber and the pH solution get to the target temperature. Fig. 11 depicts the evolution of peak intensity at the target wavelength for the different pH samples.

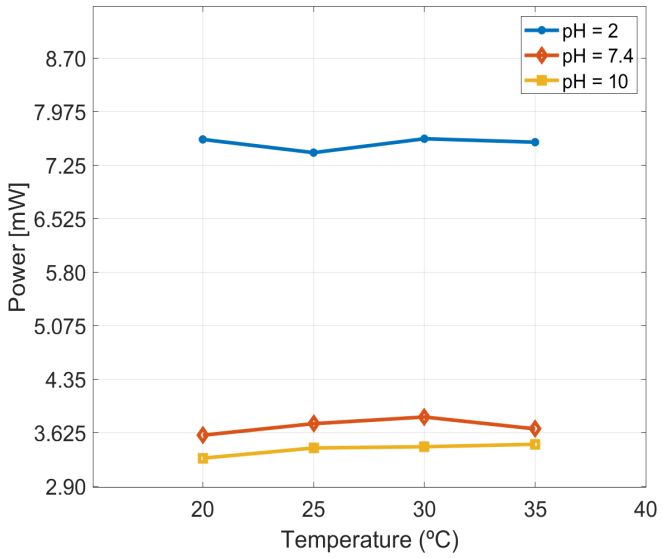

Fig. 12. Temperature variation influence in the D-shape fiber-based sensor.

The most significative changes are observed for temperatures below 25 °C for all the samples, where the peak intensity changes abruptly. This is possible to occur due to the interaction of the thermal stabilization mechanism inside the chamber and the reaction of PAni with the pH samples.

The TCFF type of pH sensor has demonstrated an optimal temperature operation range above 25 °C and can be adjusted according to application requirements.

In the case of D-shape fiber-based sensor, the temperature has practically no influence on the sensor response, as depicted in Fig. 12. A high stability is achieved in the full operation range.

E. Discussion

To provide context and highlight the performance of the proposed TCFF and D-shape fiber pH sensors in relation to other state-of-the-art technologies, Table I describes a summarized comparative analysis. Both the TCFF and D-shape optical fiber sensors offer competitive measurement ranges, covering the acidic to neutral/slightly alkaline pH regimes relevant for many environmental monitoring and industrial process control applications.

When compared to other pH sensing technologies listed in Table I, such as electrochemical (potentiometric and ISFET), optical (SPR and fluorescence), and nanomaterial-based approaches, the proposed optical fiber sensors offer several advantages. However, it is important to acknowledge some limitations and areas for further improvement. The development of robust packaging and probe designs will be crucial for practical deployments in various application scenarios.

IV. Conclusion

In this work, two optical fiber pH sensors using a TCFF and a D-shape fiber, both coated with PAni polymer, were presented. This layer was produced in situ by coating the optical fiber surface via synthetic oxidative polymerization.

TABLE I
Comparative Analysis of the Proposed Optical Fiber pH Sensors With Other State-of-the-Art Technologies

Sensor Type	Sensing mechanism	Sensitivity	Ref
ISFET	AlN gate-based sensor	-33 mV/pH	[23]
Potentiometric	PAni-based sensor	-62.3 mV/pH	[24]
	Nb/Nb_2O_5 electrode	-41 mV/pH	[25]
Embedded in optical fiber	Coated etched LPG	-0.173 nm/pH	[26]
	Al/Pt-coated unclad core optical fiber	-2.77 nm/pH	[27]
	Coated POF-inscribed FBG	-0.34 nm/pH	[15]
	TCFF (this work)	1.06 mW/pH	-
	D-shape fiber (this work)	0.95 mW/pH	-

The sensors achieved a variable sensitivity response, where the optimal operation zone, matching a linear trend, was between pH 4.2 and 8.1. In this range, the sensitivity measured was 1.06 mW/pH in terms of peak intensity for the trenched only-bridge optical fiber.

The results were compared to the side-polished D-shaped fiber sensor. In this case, the linear sensitivity range was from 2.75 to 6.8, where the maximum variation achieved was 0.95 mW/pH.

The sensors were analyzed in multiple usages. The test was repeated on different days to check the response regarding the quality of PAni coating after polymerization time. The trenched only-bridge optical fiber showed the best response in terms of normalized transmittance, which increased around 10% after the third test. However, the D-shape fiber achieved a significative change in pH levels above 7.1.

In terms of environmental cross-sensitivity, both sensors recorded did not show significant spectral response under temperature changes. In the case of THCF-based sensor, a slight variation in peak power intensity was recorded for temperatures under 25 °C, due to possible stabilization time mismatches.

The proposed sensor configurations can be further improved by combining both sensors and covering a higher range of pH measurements. The D-shape fiber for the low-pH zone and the TCFF for the high-pH zone, making a full pH 2.75–8.1 range. Moreover, in terms of cost-effectiveness of the system, the measurements can be performed using power meters to check the signal intensity losses as the pH increases.

Acknowledgment

Armando Rodriguez, Mikel Bravo, and Manuel Lopez-Amo are with the Electrical, Electronic and Communication Engineering Department and the Institute of Smart Cities (ISC), Public University of Navarra, 31006 Pamplona, Spain (e-mail: armando.rodriguez@unavarra.es).

Guilherme Lopes is with CICECO, Physics Department, University of Aveiro, 3810-193 Aveiro, Portugal.

Jan Nedoma is with the Department of Telecommunications, VSB–Technical University of Ostrava, 708 00 Ostrava, Czech Republic.

Sónia O. Pereira and António J. S. Fernandes are with I3N, Physics Department, University of Aveiro, 3810-193 Aveiro, Portugal.

Raphael Jamier and Philippe Roy are with XLIM UMR CNRS 7252, University of Limoges, 87000 Limoges, France.

Carlos Marques is with CICECO, Physics Department, University of Aveiro, 3810-193 Aveiro, Portugal, and also with the Department of Physics, VSB–Technical University of Ostrava, 70800 Ostrava, Czech Republic.

REFERENCES

[1] J. Werner, M. Belz, K.-F. Klein, T. Sun, and K. T. V. Grattan, "Fiber optic sensor designs and luminescence-based methods for the detection of oxygen and pH measurement," *Measurement*, vol. 178, Jun. 2021, Art. no. 109323, doi: 10.1016/j.measurement.2021.109323.

[2] P. Gou et al., "Carbon nanotube chemiresistor for wireless pH sensing," *Sci. Rep.*, vol. 4, no. 1, p. 4468, Mar. 2014, doi: 10.1038/srep04468.

[3] V. Perumal, "pH measurement using in house fabricated interdigitated capacitive transducer," in *Proc. RSM*, 2013, pp. 2–4.

[4] L. Manjakkal, S. Dervin, and R. Dahiya, "Flexible potentiometric pH sensors for wearable systems," *RSC Adv.*, vol. 10, no. 15, pp. 8594–8617, 2020, doi: 10.1039/D0RA00016G.

[5] P. Kraikaew, S. Jeanneret, Y. Soda, T. Cherubini, and E. Bakker, "Ultrasensitive seawater pH measurement by capacitive readout of potentiometric sensors," *ACS Sensors*, vol. 5, no. 3, pp. 650–654, Feb. 2020, doi: 10.1021/acssensors.0c00031.

[6] M. S. Arefin, M. Coskun, T. Alan, A. Neild, J.-M. Redoute, and M. Yuce, "A MEMS capacitive pH sensor for high acidic and basic solutions," in *Proc. IEEE Sensors*, 2014, pp. 1–3, doi: 10.1109/ICSENS.2014.6985373.

[7] Y.-Z. Juang, C.-F. Lin, H.-H. Tsai, H.-H. Liao, and R.-L. Wang, "CMOS biomedical sensor with in situ gold reference electrode for urine detection application," *Proc. Eng.*, vol. 47, pp. 1005–1008, Dec. 2012, doi: 10.1016/j.proeng.2012.09.317.

[8] S. Singh and B. D. Gupta, "Fabrication and characterization of a highly sensitive surface plasmon resonance based fiber optic pH sensor utilizing high index layer and smart hydrogel," *Sens. Actuators B, Chem.*, vol. 173, pp. 268–273, Oct. 2012, doi: 10.1016/j.snb.2012.06.089.

[9] S. K. Mishra and B. D. Gupta, "Surface plasmon resonance based fiber optic pH sensor utilizing Ag/ITO/Al/hydrogel layers," *Analyst*, vol. 138, no. 9, p. 2640, Mar. 2013, doi: 10.1039/c3an00097d.

[10] T. H. Nguyen, T. Venugopalan, T. Sun, and K. T. V. Grattan, "Intrinsic fiber optic pH sensor for measurement of pH values in the range of 0.5–6," *IEEE Sensors J.*, vol. 16, no. 4, pp. 881–887, Feb. 2016, doi: 10.1109/JSEN.2015.2490583.

[11] P. Zubiate et al., "D-shape optical fiber pH sensor based on lossy mode resonances (LMRs)," in *Proc. IEEE Sensors*, Nov. 2015, p. 4, doi: 10.1109/ICSENS.2015.7370421.

[12] J. M. Corres, I. R. Matias, I. del Villar, and F. J. Arregui, "Design of pH sensors in long-period fiber gratings using polymeric nanocoatings," *IEEE Sensors J.*, vol. 7, no. 3, pp. 455–463, Mar. 2007, doi: 10.1109/JSEN.2007.891933.

[13] Y. Zheng et al., "Miniature pH optical fiber sensor based on Fabry–Perot interferometer," *IEEE J. Sel. Topics Quantum Electron.*, vol. 22, no. 2, pp. 331–335, Mar. 2016, doi: 10.1109/JSTQE.2015.2497438.

[14] A. Leal-Junior, J. Guo, R. Min, A. J. Fernandes, A. Frizera, and C. Marques, "Photonic smart bandage for wound healing assessment," *Photon. Res.*, vol. 9, no. 3, p. 272, Mar. 2021, doi: 10.1364/PRJ.410168.

[15] X. Cheng, J. Bonefacino, B. O. Guan, and H. Y. Tam, "All-polymer fiber-optic pH sensor," *Opt. Exp.*, vol. 26, no. 11, p. 14610, May 2018, doi: 10.1364/oe.26.014610.

[16] A. L. Aldaba et al., "Polyaniline-coated tilted fiber Bragg gratings for pH sensing," *Sens. Actuators B, Chem.*, vol. 254, pp. 1087–1093, Jan. 2018, doi: 10.1016/j.snb.2017.07.167.

[17] G. Lopes et al., "Innovative optical pH sensors for the aquaculture sector: Comprehensive characterization of a cost-effective solution," *Opt. Laser Technol.*, vol. 171, Apr. 2024, Art. no. 110355, doi: 10.1016/j.optlastec.2023.110355.

[18] Y. Han et al., "Side-polished fiber as a sensor for the determination of nematic liquid crystal orientation," *Sens. Actuators B, Chem.*, vol. 196, pp. 663–669, Jun. 2014, doi: 10.1016/j.snb.2014.02.076.

[19] Y. Chen, "A review of polyaniline based materials as anodes for lithiumion batteries," *IOP Conf. Ser., Mater. Sci. Eng.*, vol. 677, no. 2, Dec. 2019, Art. no. 022115, doi: 10.1088/1757-899X/677/2/022115.

[20] M. Beygisangchin, S. Abdul Rashid, S. Shafie, A. R. Sadrolhosseini, and H. N. Lim, "Preparations, properties, and applications of polyaniline and polyaniline thin films—A review," *Polymers*, vol. 13, no. 12, p. 2003, Jun. 2021, doi: 10.3390/polym13122003.

[21] K. M. C. Tjørve and E. Tjørve, "The use of Gompertz models in growth analyses, and new gompertz-model approach: An addition to the unified-richards family," *PLoS ONE*, vol. 12, no. 6, Jun. 2017, Art. no. e0178691, doi: 10.1371/journal.pone.0178691.

[22] T. Khanikar and V. K. Singh, "PANI-PVA composite film coated optical fiber probe as a stable and highly sensitive pH sensor," *Opt. Mater.*, vol. 88, pp. 244–251, Feb. 2019, doi: 10.1016/j.optmat.2018.11.044.

[23] S. Sinha, R. Mukhiya, R. Sharma, P. K. Khanna, and V. K. Khanna, "Fabrication, characterization and electrochemical simulation of AlN-gate ISFET pH sensor," *J. Mater. Sci., Mater. Electron.*, vol. 30, no. 7, pp. 7163–7174, Apr. 2019, doi: 10.1007/s10854-019-01033-5.

[24] F. Mazzara et al., "PANI-based wearable electrochemical sensor for pH sweat monitoring," *Chemosensors*, vol. 9, no. 7, p. 169, Jul. 2021, doi: 10.3390/chemosensors9070169.

[25] T. D. Singewald, I. Traxler, G. Schimo-Aichhorn, S. Hild, and M. Valtiner, "Versatile, low-cost, non-toxic potentiometric pH-sensors based on niobium," *Sens. Bio-Sensing Res.*, vol. 35, Feb. 2022, Art. no. 100478, doi: 10.1016/j.sbsr.2022.100478.

[26] H.-Y. Wen, J.-J. Weng, and C.-C. Chiang, "PH sensor through a self-assembled multifunctional layer with clitoria ternatea based on long-period fiber gratings," *IEEE Sensors J.*, vol. 21, no. 10, pp. 12137–12145, May 2021, doi: 10.1109/JSEN.2021.3065034.

[27] I. Antohe, L.-I. Jinga, V.-A. Antohe, and G. Socol, "Sensitive pH monitoring using a polyaniline-functionalized fiber optic—Surface plasmon resonance detector," *Sensors*, vol. 21, no. 12, p. 4218, Jun. 2021, doi: 10.3390/s21124218.